DEVELOPMENT OF MULTI-POLARIZATION SAR ALGORITHM FOR SOIL MOISTURE IN CAMBODIA

PI No. 140

Kentaro Aida[1], Toshio Koike[1], Takeo Tadono[2], Jianchen Shi[3]
So Im Monichoth[4], Preap Sameng[4], Long Saravuth[4]

[1] Department of Civil Engineering, The University of Tokyo, 7-3-1, Hongo, Bunkyo-ku, Tokyo, 113-8656 Japan
Tel: +81-3-5841-6105, Fax: +81-3-5841-6130, E-mail: aida@hydra.t.u-tokyo.ac.jp
[2] Earth Observation Research Center (EORC), Japan Aerospace Exploration Agency (JAXA), Japan
[3] Institute for Computational Earth System Science (ICESS), University of California, U.S.A.
[4] Ministry of Water Resources and Meteorology (MOWRAM), Cambodia

Abstract: A Synthetic Aperture Radars (SAR) is expected to observe soil moisture with high spatial resolution in large area. Recently, some multi-polarization SAR have been in operation. The purpose of this study is to develop the algorithm to estimate soil moisture by using multi-polarization data acquired with the Phased Array type L-band Synthetic Aperture Radar (PALSAR) onboard the Advanced Land Observing Satellite (ALOS). In this study, we developed an algorithm for soil moisture estimation in the experimental field in Cambodia and showed that this algorithm can be potentially used to obtain the spatial pattern of soil moisture distribution with a 10 m spacing.

1. INTRODUCTION

In Cambodia, agriculture is an important industry that engages many people. However, only the water supplied during rainy season supports all agriculture. To use the limited water resources effectively, it is necessary to manage the water-resources based on meteorological predictions and river runoff prediction. As a factor in these predictions, soil moisture plays a key role in water and thermal transportation to the atmosphere and the contribution of river runoff properties. Knowledge of soil moisture distribution within the paddy field is beneficial for agricultural activity and management.

The SAR has high responsiveness to soil moisture. However, for a quantitative estimation of soil moisture, it is necessary to simultaneously determine the contributions of many parameters through microwave scattering. It is difficult to determine these contributions by employing single-polarization SAR. However, the PALSAR onboard the ALOS is a multi-polarization SAR that can potentially be used to determine these contributions. The aim of this study was to develop an SAR algorithm to estimate soil moisture by using the multi-polarization data acquired with PALSAR.

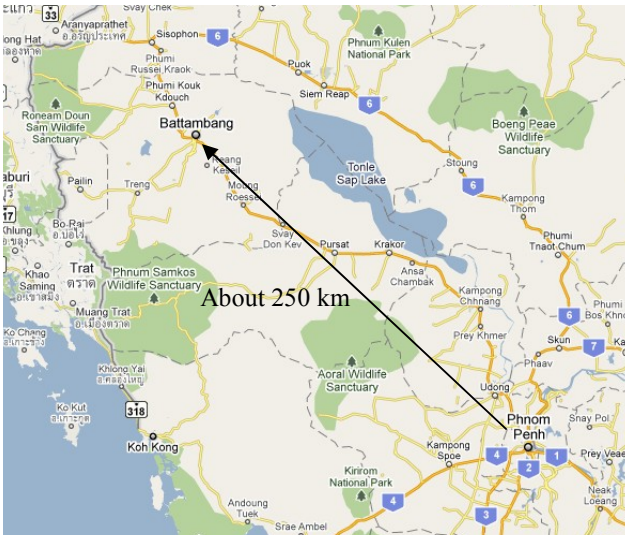

Fig. 1 Location map

$$\sigma^0 = f(\text{surface scattering}) + f(\text{volume scattering})$$

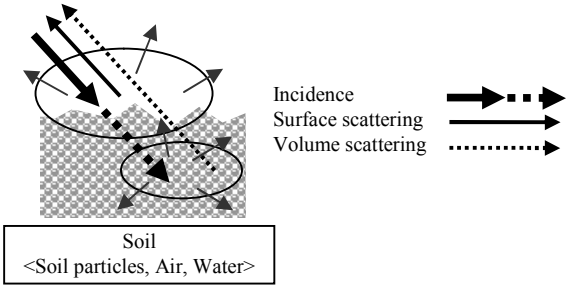

Fig. 2 Soil influence on microwave scattering

Fig. 3 Photograph of soil moisture observation

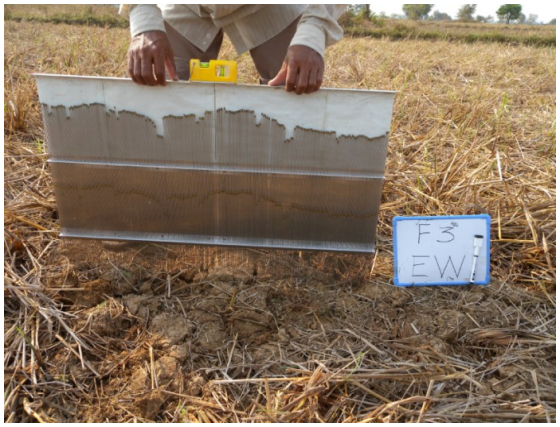

Fig. 5 Photograph of surface profile observation

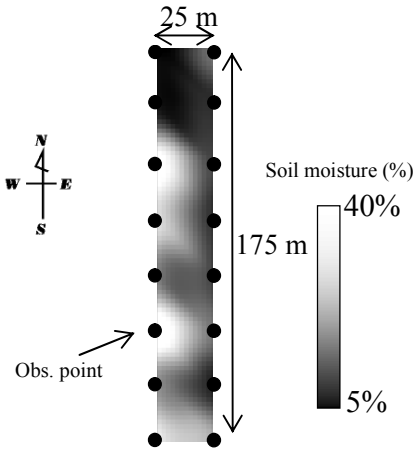

Fig. 4 Interpolated distribution of soil moisture

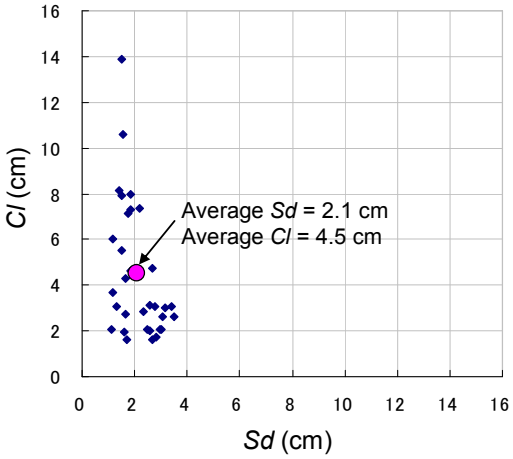

Fig. 6 Distribution of *Sd* and *Cl*.

2. RELATIONSHIP BETWEEN BACKSCATTERING COEFFICIENT AND PARAMETERS

The SAR measures the intensity of the microwaves transmitted from the satellite antenna and reflected from the earth's surface. In the level 1.5 PALSAR data, microwave intensity is expressed in terms of a backscattering coefficient (σ^0).

In general, the backscattering coefficient is a signal based on the complex interaction of the microwave scattering with not only soil moisture but also the ground surface and inside of the soil. The microwave scattering on bare ground is assumed to consist of the surface scattering and the volume scattering as shown in Fig. 2.

To simulate the microwave scattering, we used an existing numerical model developed by J. Shi *et al.* [1]. The main parameters of the model are soil moisture (*Mv*), standard deviation of surface height (*Sd*), surface correlation length (*Cl*), volume fraction of soil particles (*Sv*), and average diameter of soil particles (*D*).

The surface roughness parameters such as *Sd* and *Cl* mainly contribute to surface scattering, the soil structure parameters such as *Sv* and *D* mainly contribute to volume scattering, and the soil moisture *Mv* contributes to both types of scattering.

In this model, the relationship between σ^0 and the soil parameters can be written as

$$\sigma^0_{pq} = f(\lambda, p, q, \theta, Mv, Sd, Cl, Sv, D) \qquad (1)$$

where λ, p, q, and θ are frequency, transmission polarization, receiving polarization, and incidence angle, respectively. These parameters can be defined by the specifications of the SAR system.

3. FIELD OBSERVATIONS

We conducted three field observations synchronized with the PALSAR polarimetric mode in a paddy field in Cambodia between February and April 2010. Then, we collected field data on certain stages of rice growth. This study was subject to field observation data collected in February 2010.

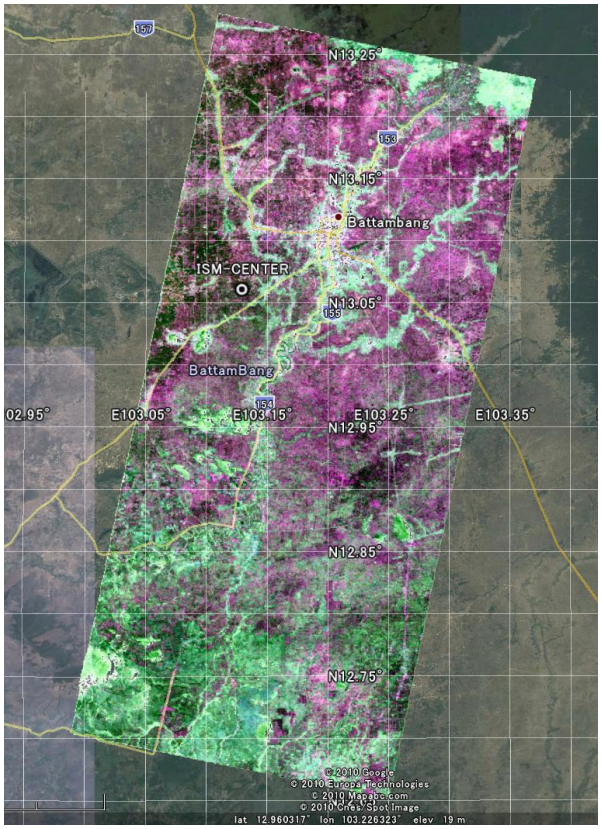

Fig. 7 Full PALSAR image (PLR mode)

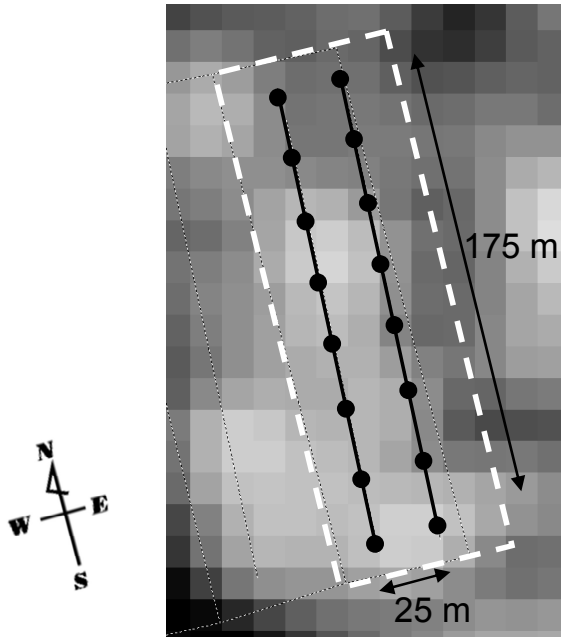

Fig. 8 Subset PALSAR image at HH polarization

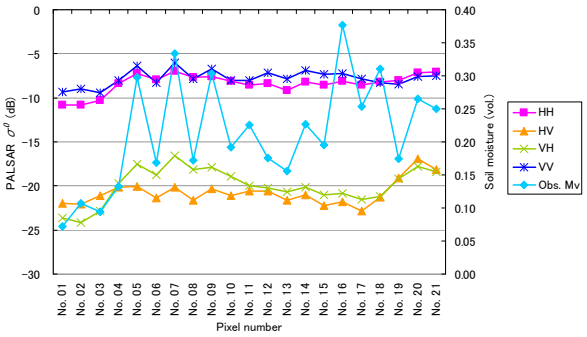

Fig. 9 Observed soil moisture and PALSAR σ^0 at reference pixels

3-1. FIELD CONDITIONS

The experimental field is located in a part of a large paddy field in a suburb of Battambang City, which is located about 250 km northwest of Phnom Penh, Cambodia, as shown in Fig.1. The field was post-harvest and covered by straw. The field surface consisted of wet soft areas and dried, hard areas that contained cracks.

The size of the experimental field was 50 m in the east-west direction and 200 m in the north-south direction. We observed *Mv*, *Sd*, and *Cl*, at 16 points at 25m intervals in the field simultaneously with the incoming of the PALSAR.

3-2. SOIL MOISTURE MEASUREMENT

To measure *Mv*, we used TRIME-FM and a P2 probe with 11cm long rods manufactured by IMKO GmbH. the probe was inserted into the soil surface perpendicularly, and therefore, the measured value is the average between 0 cm and 11 cm depth. The *Mv* values at each point are the average of three measurements around that point.

The Fig. 4 shows the spatially interpolated distribution of observed soil moisture. There was a wide range of soil moisture, from 5% to 40%, with a large spatial heterogeneity.

3-3. SURFACE ROUGHNESS MEASUREMENT

Sd and *Cl* were calculated from surface profiles measured for a width of 80 cm at 2 mm intervals using a needle-type roughness meter, as shown in Fig. 5. The surface profiles were measured twice in the north-south and east-west directions at each point.

Fig. 6 shows the distribution of *Sd* and *Cl*. The ranges of *Sd* and *Cl* are from 1 cm to 4 cm and from 1 cm to 14 cm, and the averages are 2.1 cm and 4.5 cm, respectively.

3-4. PALSAR DATA

PALSAR multi-polarization data with 12.5 m resolution was obtained at 10:30 am at the local time. The in-situ data was obtained simultaneously. Fig. 7 shows the full PALSAR image. Fig. 8 is a subset image of HH polarization corresponding to the targeted area.

In this study, we used the 21 pixels that correspond to the 175 m by 25 m targeted area inside the observation

points. Fig. 9 shows the observed soil moisture and PALSAR σ^0 of each polarization at the reference pixels. Despite the fact that the observed soil moisture is high between pixel nos. 16 and 18, there are no responses on PALSAR σ^0.

4. IDENTIFICATION OF PARAMETERS

This study used HH, VH, and VV polarizations, which are computable on the numerical model. Eq. 1 is rewritten for different polarizations excepting parameters defined by the specifications of SAR, as Eq. 2.

$$\begin{aligned} \sigma^0_{HH} &= f(Mv, Sd, Cl, Sv, D) \\ \sigma^0_{VH} &= f(Mv, Sd, Cl, Sv, D) \\ \sigma^0_{VV} &= f(Mv, Sd, Cl, Sv, D) \end{aligned} \quad (2)$$

There are five unknown parameters in σ^0 at three polarizations. If two parameters are know, the other three parameters may be found by solving these equations using multi-polarization data.

In this study, *Sv* and *D* were considered adjustable parameters because their measurement in the fields is difficult, we assumed that these parameters were uniform in similar areas. The values of both parameters were derived by calculating σ^0 with numerical model simulations using *Mv*, *Sd*, and *Cl* collected in field observations. With regard to *Sd* and *Cl*, the average was used for simplifying the identification of adjustable parameters without considering the spatial distribution. According to our simulation using the numerical model, the contribution of *Sd* and *Cl* to microwave scattering is smaller than the contribution of soil moisture. By dividing the soil moisture into four categories, 0–9%, 10–19%, 20–29%, and 30% and above, optimized sets of *Sv* and *D* were obtained, as shown in Table 1. Fig. 10 shows the result of the tuning at different polarizations within each category. The values of simulated σ^0 and PALSAR σ^0 appear to be in good agreement.

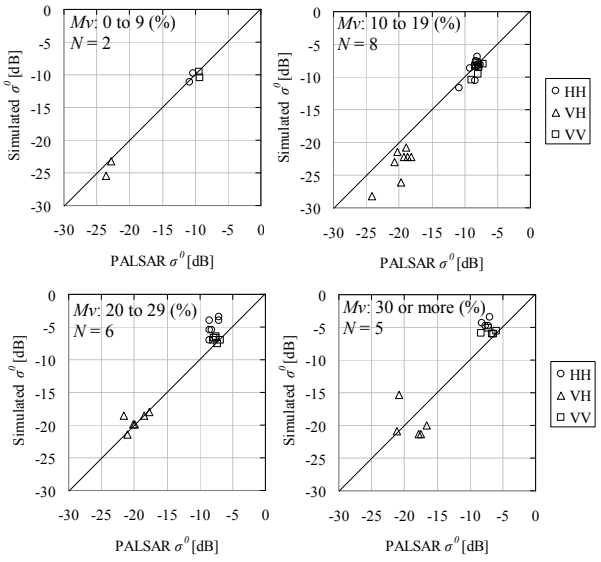

Fig. 10 Results of tuning at different polarization

5. CONSTRUCTION OF LOOKUP TABLE

Then, we obtained the relationship between the parameters and the multi-polarization σ^0, and subsequently constructed the lookup table to estimate soil moisture from the multi-polarization PALSAR data.

This lookup table is that the sets of the parameters calculated by the numerical model are distributed at three-dimensional space where the axes consist of each σ^0 such as HH, VH, and VV polarization in dB. By introducing the observed σ^0 at different polarization, and getting the nearest point value from the lookup table, we can estimate *Mv*, *Sd*, and *Cl*.

Table 2 shows the range of the parameters in the lookup table.

Table 1 Optimized sets of *Sv* and *D*

Mv (%)	*Sv* (vol.)	*D* (cm)
0–9	0.6	1.4
10–19	0.2	1.0
20–29	0.2	0.9
30 and above	0.2	0.6

Table 2 Range of parameters in lookup table

Parameter	Range	Interval
Mv (%)	1.0–60.0	2.0
Sd (cm)	0.1–3.5	0.5
Cl (cm)	0.1–20.0	2.5
Sv (vol.)	Depends on *Mv*	-
D (cm)	Depends on *Mv*	-
Incidence angle (deg.)	24.5	-

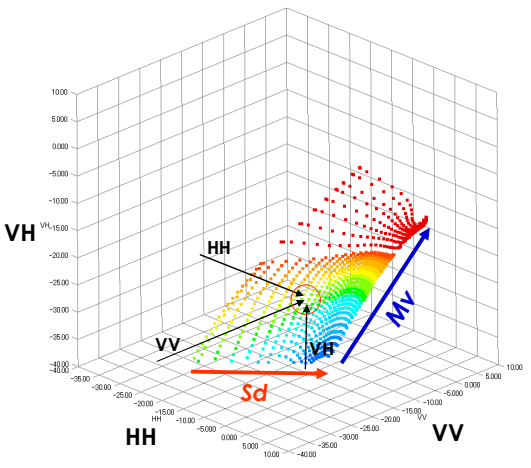

Fig. 11 Virtual image of lookup table

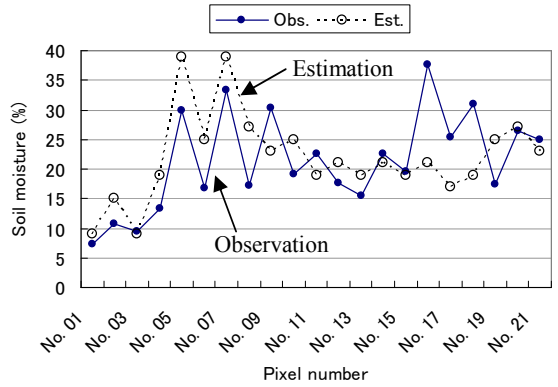

Fig. 12 Result of soil moisture estimation

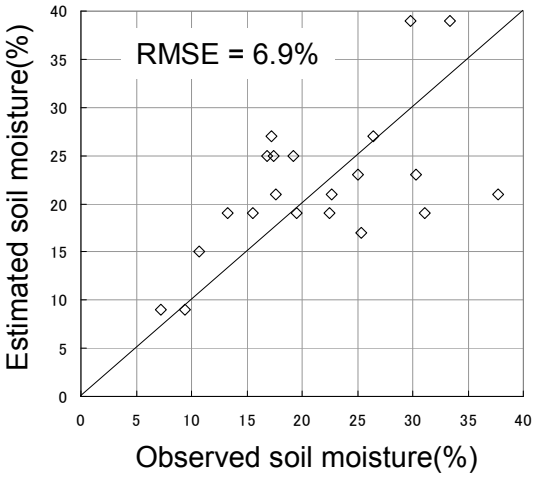

Fig. 13 Comparison between observed and estimated soil moisture

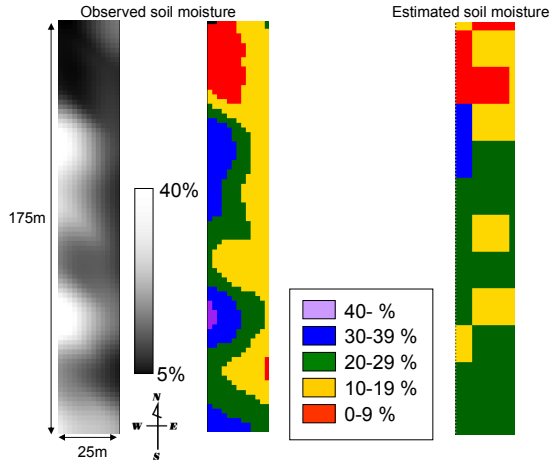

Fig. 14 Spatial pattern of soil moisture distribution

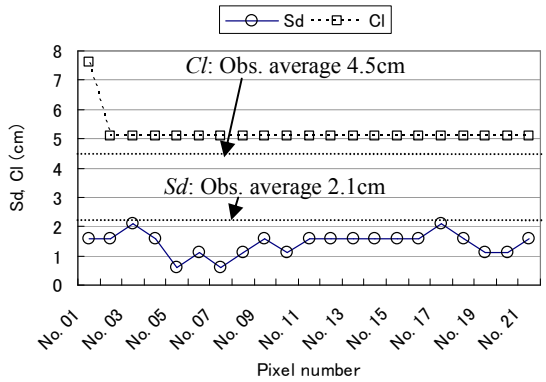

Fig. 15 Result of surface roughness parameters estimation

6. RESULTS OF ESTIMATION

Fig. 12 shows the result of the soil moisture estimation in the paddy field. In the result, there is a large error between pixel nos. 16 and 18, and the RMSE is 6.9%. One reason for the large error is that the actual soil moisture was not distributed as widely as the interpolated distribution. However, the trend of soil moisture distribution is expressed very accurately. The spatial pattern of the soil moisture distribution from the algorithm corresponds to the observed one as shown in Fig. 14.

Fig. 15 shows the result of the estimation of roughness parameters such as *Sd* and *Cl*. The error between the estimated values and the average of the observed values at almost points are less than 1 cm.

7. CONCLUSION

In this study, we developed an algorithm for soil moisture estimation in the experimental field and showed that this algorithm can be potentially used to obtain the spatial pattern of soil moisture distribution with a 10 m spacing. As a next step, we will try to extend this technique to an entire paddy field. There are several types of soil in the paddy field of Cambodia [2], therefore, we have to consider whether *Sv* and *D* optimized in this experimental field can be applied to other paddy fields. To identify *Sv* and *D*, the field observations need to be synchronized with PALSAR polarimetric mode in each type of soil, and the relationship between σ^0 and the parameters must be considered.

Once a distribution map of the parameters, excluding *Mv*, is obtained using multi-polarization SAR data, it is expected that soil moisture estimation from single-polarization SAR data acquired with the ScanSAR mode for observation of a larger area and the FBS mode for observation in greater detail, will be possible. Table 3 shows the observation modes of PALSAR.

Table 4 shows a list of C-band SARs in operation. If this algorithm is applied to the presently operational C-band SARs such as ERS-2, RADARSAT-1 and 2, and ENVISAT, the frequency of soil moisture mapping by SAR is expected to increase significantly.

Table 3 Observation modes of PALSAR

Observation mode	Polarization	Resolution
Fine (FBS)	HH / VV	6.25 m
Fine (FBD)	HH + HV / VH + VV	12.5 m
ScanSAR	HH / VV	100 m
Polarimetric (PLR)	HH + HV + VH + VV	12.5 m
Frequency: L-band(1.27 GHz) Wave length: 23.6 cm		

Table 4 List of C-band SARs in operation

Name	Band	Polarization	Operation	Facilities
ERS-2/SAR	C	Single pol.	Apr 1995	ESA
RADARSAT-1	C	Single pol.	Nov 1995	CSA
ENVISAT/ASAR	C	Dual pol.	Mar 2002	ESA
RADARSAT-2	C	Quad pol.	Dec 2007	CSA

ACKNOWLEDGMENTS

This study was conducted under the Space Applications for Environment (SAFE) project. The authors thank the JAXA for providing the PALSAR data used in this study, and the MOWRAM for the support with the field observations.

REFERENCES

[1] Jiancheng Shi, James Wang, Ann Y. Hsu, Peggy E. O'Neil, and Edwin T. Engman, "Estimation of bare surface soil moisture and surface roughness parameters using L-band SAR Image Data," *IEEE Trans. Geosci. and Remote Sensing*, Vol. 35, No. 5, pp. 1254-1264, 1997.

[2] "The Atlas of Cambodia National Poverty and Environment Maps," Save Cambodia's Wildlife, Phnom Penh, Cambodia, 2006.